PROCEEDINGS OF SPIE

SPIEDigitalLibrary.org/conference-proceedings-of-spie

Effects of tissue autofluorescence on FRET efficiency estimates

Pleshinger, D. J., Annamdevula, Naga, Leavesley, Silas, Rich, Thomas

D. J. Pleshinger, Naga Annamdevula, Silas J. Leavesley, Thomas C. Rich, "Effects of tissue autofluorescence on FRET efficiency estimates," Proc. SPIE 11649, Three-Dimensional and Multidimensional Microscopy: Image Acquisition and Processing XXVIII, 1164919 (5 March 2021); doi: 10.1117/12.2583284



Event: SPIE BiOS, 2021, Online Only

Effects of tissue autofluorescence on FRET efficiency estimates

D.J. Pleshinger^{ab}, Naga Annamdevula^{ab}, Silas J. Leavesley^{abc}, and Thomas C. Rich^{ab}

^aDepartment of Pharmacology, University of South Alabama ^bCenter for Lung Biology, University of South Alabama ^cDepartment of Chemical and Biomolecular Engineering, University of South Alabama

ABSTRACT

Förster resonance energy transfer (FRET) is a tool used for studying various biological process as well as for measuring molecular distances. This process can occur when the emission spectrum of the donor fluorophore overlaps with the excitation spectrum of the acceptor, and the fluorophores are in close enough distance for the energy to pass from donor to acceptor non-radiatively. The efficiency of this energy transfer is dependent on the distance and orientation of the fluorophores, in addition to their overlapping spectra. Here we present a study to assess the impact of tissue autofluorescence on estimates of FRET efficiency and fluorophore abundance within experimental cellular images in tissue. To accomplish this we performed a theoretical sensitivity analysis on FRET rat kidney control images with varying ranges of donor and acceptor fluorophores to observe their pixel by pixel responses. In the experimental data, the donor was the Turquoise fluorescent protein and the acceptor fluorophore was the Venus fluorescent protein. Detection of the acceptor was more difficult due to its excitation spectrum closely resembling the autofluorescence spectrum from the base image while the emission spectrum of the Turquoise donor was more unique and easier to detect. In addition, variable FRET efficiencies were added to data at different fluorophore levels to compare the visible abundance of FRET to the autofluorescence in the resultant images. This analysis can benefit future work by furthering the understanding of the donor and acceptor concentrations needed for strong FRET measurements.

Keywords: Autofluorescence, FRET, Spectral Imaging

1. INTRODUCTION

Förster resonance energy transfer (FRET) is a process by which energy is transferred from an excited, donor fluorophore to an acceptor fluorophore 1. This non radiative process can occur when the molecules are separated by 1-10 nm and there is overlap between the emission spectrum of the donor and the excitation spectrum of the acceptor 2,3. The efficiency of FRET is a result of the distance between the fluorophores and their spectra.

Another factor that is critical for FRET measurements is the autofluorescence signal from the sample being imaged 4,5. While the distance and spectra of the donor and acceptor fluorophores directly affect the FRET efficiency, the ability to unmix, detect and quantify the fluorophore signals in the presence of background autofluorescence is crucial for accurate FRET measurements in cells and tissues. Keeping this in mind, the relative abundance of fluorophores needs to be considered when designing experiments.

2. METHODS

2.1 Data Acquisition

The images used for this theoretical sensitivity study were of kidney slices from Sprague Dawley rats. Imaging was conducted using a Nikon A1R spectral confocal microscope. Samples were excited using 405 nm excitation laser and the emission was collected at wavelengths ranging from 414 nm - 724 nm with 10 nm intervals. Spectral data were exported to individual -.tif images using Nikon Elements software. Each image corresponds to a single band pass. A band sequential image (.bsq) was generated from -.tif files using MATLAB programming environment, and this -.bsq file was used for the analysis.

Further author information: (Send correspondence to D.J.P.)

D.J.P.: E-mail: djpleshinger@southalabama.edu

Three-Dimensional and Multidimensional Microscopy: Image Acquisition and Processing XXVIII, edited by Thomas G. Brown, Tony Wilson, Laura Waller, Proc. of SPIE Vol. 11649, 1164919 © 2021 SPIE · CCC code: 1605-7422/21/\$21 · doi: 10.1117/12.2583284

2.2 Image Analysis

Analysis was performed using custom MATLAB scripts to produce two main results. First, a Theoretical Sensitivity Curve (TSC) was produced for both the acceptor and donor spectra by adding scaled amounts or each spectra to a region of interest (ROI) within the image. This curve will show how the intensity of the unmixed pixels in the ROI change with the varying amounts of scaled spectra. The ROI was chosen to be a location where there was higher autofluorescence that would be more likely to affect the observed FRET signal. For this theoretical look a small square region was chosen for simplicity and faster computational time.

Unmixing of the images was performed in MATLAB using normalized donor and acceptor libraries described in 6 along with an ImageJ calculated autofluorescence spectrum. Figure 1 displays the normalized spectra on the left and the actual spectra used for unmixing on the right. The normalized Venus was reduced further due to a FRET correction described by Naga et. al. in 6. The TSC plotted in Figure 2 and described in Section 3 show the intensities of the pixels in the ROI versus the scaled amounts of the added endmember. A linear fit based on the average of each scaled amount is shown with a black line, with standard deviations shown in red.

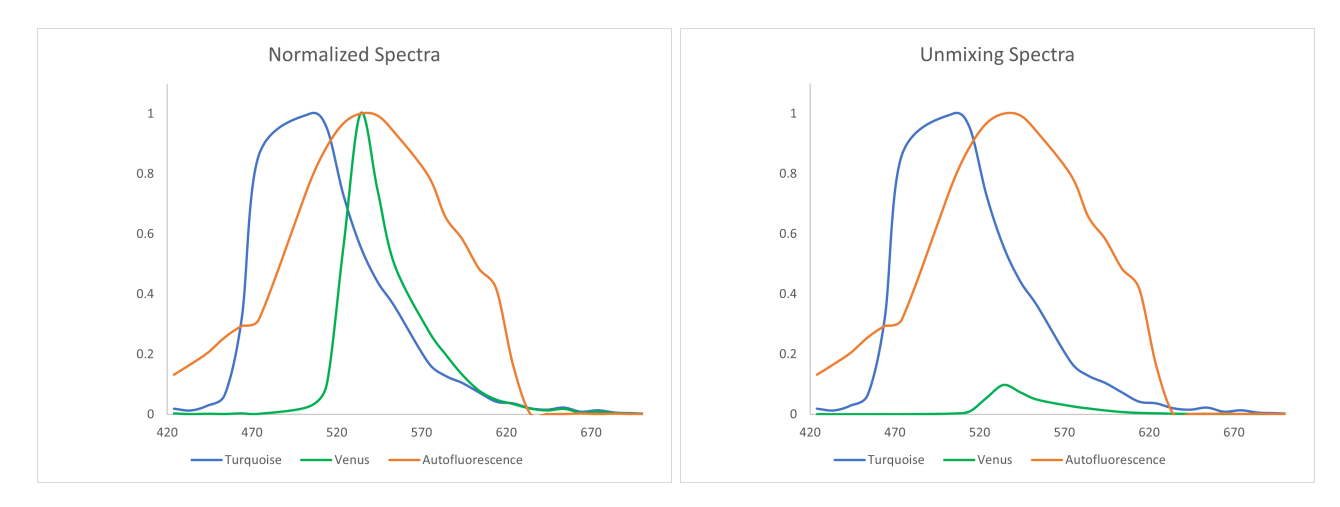


Figure 1. The caption.

Unmixed images of zero, low, and high FRET efficiencies per pixel were produced by adding set amounts of the donor and acceptor spectra for the desired FRET efficiencies. We ensured that the donor and acceptor fluorophore would be discernable from background using data from the TSC curves. Using scaled values determined from the TSC for the Turquoise endmember and a set 20% and 80% FRET efficiency, the amount of the Venus spectrum that was needed to be added was calculated from

$$FE = \frac{(A-D)}{A+17.128*D} \tag{1}$$

where FE is the FRET Efficiency of a pixel, A is the unmixed acceptor value and D is the unmixed donor value. The scaled value of the donor and acceptor spectra were then added to the ROI. Images were unmixed using the spectra described above, and FRET efficiencies were calculated for each pixel from the unmixed donor and acceptor images.

3. RESULTS AND DISCUSSION

The theoretical sensitivity analysis of the donor and acceptor spectra produced similarly linear results; however, a distinct difference was observed in the scales of the endmembers. For the acceptor fluorophore, Figure 2, left panel, the spectrum needed to be scaled \geq 10-fold that of the donor fluorophore to produce a linear result seen in Figure 2, right panel.

This difference is a result of the similarities between the Venus and autofluorescence, Figure 1. The overlapping Venus and autofluorescence spectra make it more difficult to unmix. In this case the Turquoise (donor) signal

and the autofluorescence signal can be detected above the background more easily than the Venus (acceptor) signal. These data demonstrate that the choice of donor and acceptor fluorophores for FRET measurements in tissues is crucial, and the optimal FRET pair may be different in different tissues.

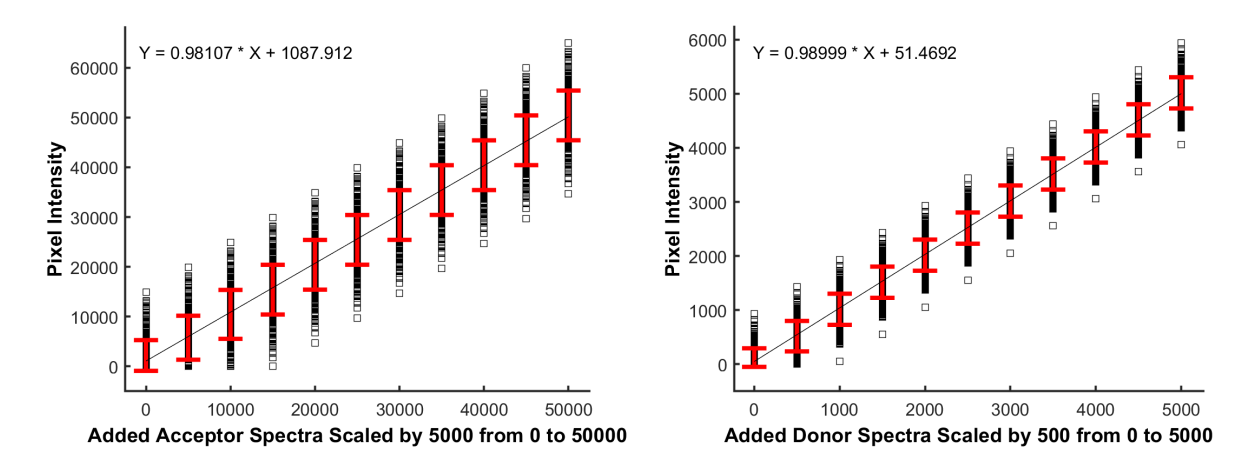


Figure 2. The TSC show ROI pixels as black squares with scaled amounts of acceptor (left) and donor (right) spectra added. Standard deviations and fit line are shown with red bars and black line respectively.

Our data demonstrate that estimates of FRET efficiency can be directly affected by tissue autofluorescence. Images of the FRET efficiency in the tissue were produced adding Turquoise and Venus at 20% and 80% efficiency. Initially, a scaled amount for the Venus was chosen from the TSC so that the lower intensity pixels would still be bright enough to be detected above the background. Once this value was chosen, the Turquoise amount added was calculated using the FRET efficiencies chosen. However, the resulting ROI was mostly 0% FRET efficiencies. This was a result due to the calculated donor amount being added still being too low for detection even while the Turquoise amount was scaled as needed.

The images seen in Figure 3 were then produced by selecting scaled values of both the donor and acceptor endmember that corresponded with the 20% and 80% FRET efficiencies desired. Here it is shown in the bottom row that at 20% FRET the ROI is still similar to the background autofluorescence signal, while up at 80% the region is distinctly observable. While producing an ROI at the desired FRET efficiency has been shown, the autofluorescence of the tissue creates a unique challenge in selecting the endmembers and their intensity to be added to the sample for such results.

4. FUTURE WORK

Determining and cataloging the endmembers desired for specific tissues to produce optimal FRET signals is a critical step in intrivital FRET microscopy. Here we have shown a theoretical method of analyzing the endmember signals required in order to produce FRET observations discernable from the autofluorescence in control rat kidney images. In future work, we will apply this theoretical technique to various other tissues, such as lung and brain, to observe how their signals of different endmembers appear in comparison with their unique autofluorescence signals. This approach will then move to be validated by using transgenic rat models stably expressing FRET-based probes rather than the control images used in this work.

ACKNOWLEDGMENTS

We would like to thank Kees Jalink for providing the H188 and H187 FRET probes. This work was supported by NIH grand awards P01-HL066299, R01HL058506, and 1R01HL137030, as well as NSF grand award 1725937.

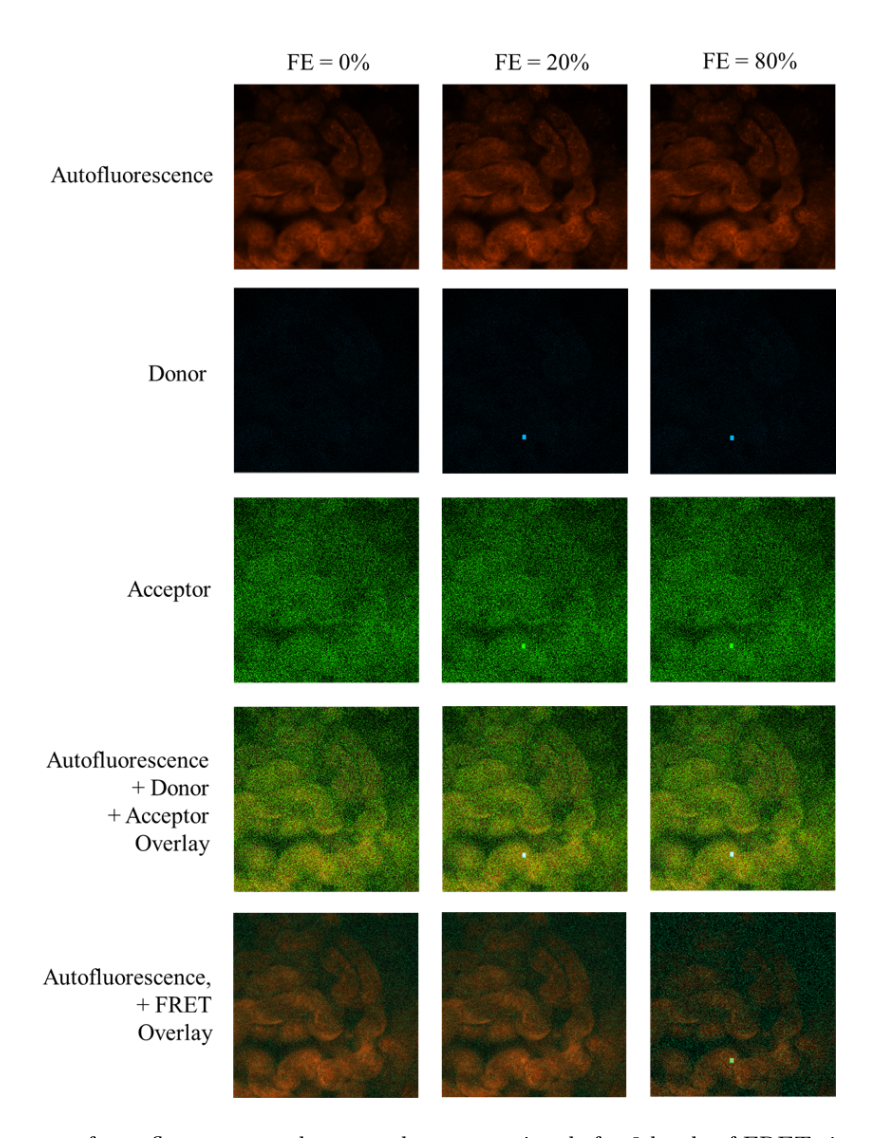


Figure 3. Unmixed images of autofluorescence, donor, and acceptor signals for 3 levels of FRET signal added to an ROI are shown in the top three rows. The fourth row shows an overlay of the autofluorescence, donor, and acceptor and the fifth row showing an overlay of the FRET signal with the autofluorescence. The ROI used for this analysis is the small square seen just to the left of center in the lower third of the images.

REFERENCES

- [1] Förster, T., "Zwischenmolekulare energiewanderung und fluoreszenz," Annalen der Physik 437(1-2), 55–75 (1948).
- [2] Clegg, R. M., "The history of FRET," Reviews in Fluorescence 2006, 1–45 (2006).
- [3] Lakowicz, J. R., "Principles of fluorescence spectroscopy," Springer US, 3rd ed. (2006).
- [4] Monici, M., "Cell and tissue autofluorescence research and diagnostic applications," *Biotechnology Annual Review* 11, 227–256, Elsevier (2005).
- [5] Hirata, E. and Kiyokawa, E., "Future perspective of single-molecule fret biosensors and intravital fret microscopy," *Biophysical Journal* **111**(6), 1103–1111 (2016).
- [6] Annamdevula, N. S., Sweat, R., Griswold, J. R., Trinh, K., Hoffman, C., West, S., Deal, J., Britain, A. L., Jalink, K., Rich, T. C., and Leavesley, S. J., "Spectral imaging of fret-based sensors reveals sustained camp gradients in three spatial dimensions," Cytometry Part A 93(10), 1029–1038 (2018).